Effects of Flow Rate on Sensitivity and Affinity in Flow Injection Biosensor Systems Studied by 55-MHz Wireless Quartz Crystal Microbalance

ARTICLE *in* ANALYTICAL CHEMISTRY · AUGUST 2008

Impact Factor: 5.64 · DOI: 10.1021/ac800459g · Source: PubMed

6 AUTHORS, INCLUDING:

Masahiko Hirao
Osaka University
302 PUBLICATIONS **2,904** CITATIONS

Anal. Chem. **2008,** *80,* 5494–5500

Effects of Flow Rate on Sensitivity and Affinity in Flow Injection Biosensor Systems Studied by 55-MHz Wireless Quartz Crystal Microbalance

Hirotsugu Ogi,*,† Yuji Fukunishi,† Toshinobu Omori,† Kenichi Hatanaka,† Masahiko Hirao,† and Masayoshi Nishiyama‡

Graduate School of Engineering Science, Osaka University, Toyonaka, Osaka, 560-8531, Japan, and Renovation Center of Instruments for Science Education and Technology, Osaka University, Machikaneyama 1-2, Toyonaka, Osaka 560-8531, Japan

In this paper, we developed a 55-MHz wireless−electrodeless quartz crystal microbalance (QCM) and systematically studied the effects of flow rate on the sensitivity to the detection of proteins and on the affinity between biomolecules evaluated by the flow injection system. Brownian motion of proteins in liquid suggests a low probability of meeting, and the convection effect plays an important role in the sensitivity and the affinity in the flow cell injection system. The wireless quartz crystal was isolated in the QCM cell, and flow rates between 50 and 1000 μL/min were used for monitoring binding reactions between human immunoglobulin G and *Staphylococcus aureus* protein A. The sensitivity was significantly increased as the flow rate increased, while the affinity value remained unchanged. However, the affinity value was affected by the reaction time for a large-concentration analyte, indicating the need of a high-sensitivity biosensor system for accurate evaluation of affinity. The electrode effect on the QCM sensitivity was also theoretically investigated, showing that the electrode significantly deteriorates the QCM sensitivity and makes the Sauerbrey equation invalid.

The importance of the affinity measurement among various biomolecules has been recognized during progress in protein design and development of drugs. Various tag proteins have been reported for affinity evaluation and purification to product recombinant proteins. However, conventional affinity tag systems use large-size tag proteins such as green-fluorescent proteins (∼>27 kDa), FLAGs with specific antibodies (∼>150 kDa), and quantum dots (>∼20 Å)[1,2] and have influence on the apparent affinity among biomolecules. Furthermore, individual affinity tags require specific buffer conditions, which will affect functions of examined proteins.[3] Therefore, significant efforts have been paid for developing small-size tags, which do not affect the functions of proteins of interest.[4,5]

The label-free methods are then important for studying inherent interactions of biomolecules. Two methods are widely recognized. One is the surface plasmon resonance (SPR) biosensor.[6–8] A conventional SPR measurement monitors interactions between a receptor protein and an analyte injected in a flow injection system. The receptor is immobilized on a metallic thin film deposited on a glass plate, which is irradiated from the back surface through a prism by a light. The coupling condition (the resonance condition) between the evanescent field generated by the incident light and the propagating surface plasmon wave at the metallic film is affected by the macroscopic electric properties in the evanescent field, and the incident angle of the light for SPR changes during the binding reaction between proteins. Monitoring the incident angle as the binding reaction progresses enables evaluation of kinetics of reactions between the molecules. The other is the quartz crystal microbalance (QCM) biosensor.[9–15] It allows determination of the mass of adsorbed proteins on the receptor immobilized on a quartz oscillator through the decrease of the resonance frequency (f),[16,17] realizing a real-time monitoring of association and dissociation reactions between molecules. Because the fractional-frequency change ($\Delta f/f$) equals the ratio of the adsorbed mass to the oscillator mass, the QCM biosensor allows quantitative measurement for the binding rate and affinity

* To whom correspondence should be addressed. Tel. +81-6 + 6850-6187. Fax: +81-6-6850-6187. E-mail: ogi@me.es.osaka-u.ac.jp.

† Graduate School of Engineering Science.

‡ Renovation Center of Instruments for Science Education and Technology.

(1) Green, M. *Angew. Chem., Int. Ed.* **2004**, *43*, 4129–4131.
(2) Bruchez, M.; Moronne, M.; Gin, P.; Weiss, S.; Alivisatos, A. *Science* **1998**, *281*, 2013–2016.
(3) Terpe, K. *Appl. Microbiol. Biotechnol.* **2003**, *60*, 523–533.
(4) Guignet, E.; Hovius, R.; Vogel, H. *Nat. Biotechnol.* **2004**, *22*, 440–444.
(5) Ojida, A.; Honda, K.; Shinmi, D.; Kiyonaka, S.; Mori, Y.; Hamachi, I. *J. Am. Chem. Soc.* **2006**, *128*, 10452–10459.
(6) Kurita, R.; Yokota, Y.; Ueda, A.; Niwa, O. *Anal. Chem.* **2007**, *79*, 9572–9576.
(7) Nedelkov, D. *Anal. Chem.* **2007**, *79*, 5987–5990.
(8) Hoaa, X.; Kirk, A.; Tabrizian, M. *Biosens. Bioelectron.* **2007**, *23*, 151–160.
(9) Muramatsu, H.; Dicks, M.; Tamiya, E.; Karube, I. *Anal. Chem.* **1987**, *59*, 2760–2763.
(10) Liu, Y.; Yu, X.; Zhao, R.; Shangguan, D.; Bo, Z.; Liu., G. *Biosens. Bioelectron* **2003**, *19*, 9–19.
(11) Ogi, H.; Motohisa, K.; Matsumoto, T.; Hatanaka, K.; Hirao, M. *Anal. Chem.* **2006**, *78*, 6903–6909.
(12) Ogi, H.; Motohisa, K.; Hatanaka, K.; Ohmori, T.; Hirao, M.; Nishiyama, M. *Biosens. Bioelectron.* **2007**, *22*, 3238–3242.
(13) Pei, Y.; Yu, H.; Pei, Z.; Theurer, M.; Ammer, C.; Andre, S.; Gabius, H.-J.; Yan, M.; Ramstrom, O. *Anal. Chem.* **2007**, *79*, 6897–6902.
(14) Shen, Z.; Huang, M.; Xiao, C.; Zhang, Y.; Zeng, X.; Wang, P. G. *Anal. Chem.* **2007**, *79*, 2312–2319.
(15) Furusawa, H.; Takano, H.; Okahata, Y. *Anal. Chem.* **2008**, *80*, 1005–1011.
(16) Sauerbrey, G. *Z. Phys.* **1959**, *155*, 206–222.
(17) Eddowes, M. J. *Biosensors* **1987**, *3*, 1–15.

10.1021/ac800459g CCC: $40.75
Published on Web 06/14/2008

without calibrations. The viscosity effect participates in the frequency shift, but it becomes less significant at higher frequencies.[18,19] Even for a low-frequency QCM, a quantitative analysis is possible by simultaneously measuring frequency and energy dissipation at multiple harmonics using a Voight-based viscoelastic model.[20] The most important advantage of the QCM biosensor is thus the quantitative nature, while the SPR measurement involves ambiguity regarding the relationship between the incident angle and the amount of the adsorbed proteins. Systematic and quantitative comparisons between QCM and SPR appear in detail elsewhere.[21,22]

These label-free biosensors have to measure quite small changes in physical quantities caused by biomolecules. Changes in resonance frequency observed in conventional QCMs are typically smaller than 0.001%, for example. Flow injection systems have been then adopted: A surface-modified sensor is set in a flow channel, and a carrier solution steadily flows through the sensor surface. When the physical response becomes stable enough, the analyte is injected. The relative change in the physical property is then detected to evaluate the kinetics of the reaction. Because of the relative change from the steady condition, high-sensitivity detection of the analyte is possible. However, in the evaluation of affinity, we have to consider the effect of the flow rate, because the convection flow will play an important role in the reaction compared with the self-diffusion of molecules. The important advantage of the flow injection system is that it allows us to assume constant concentration of the analyte during reaction, making the thermodynamic analysis easy and accurate. The analyte concentration, however, decreases and increases at the local sensor surface region in the case of association and dissociation reactions, respectively. Brownian motion is not dominant compared with the reaction time, and the convection makes the concentration of the surrounding solution recover. Thus, the sensitivity and apparent affinity may be dependent on the flow rate, and it is important to investigate this effect quantitatively.

There are three purposes in this study. First, we establish a 55-MHz wireless−electrodess QCM. Previously, we suggested significant influence of electrodes on quartz surfaces on the QCM sensitivity and proposed a noncontacting measurement of the resonance frequency for electrodess quartz plates by the line antenna.[11,12,23] The affinity has to be evaluated using lower-concentration solutions to avoid steric hindrance among biomolecules as shown later, and a high-sensitivity QCM is required. Because the QCM sensitivity increases as the thickness of the oscillator decreases, we here develop the noncontacting method for the 30-μm-thick AT-cut quartz and achieve a 55-MHz wireless QCM. Using the specific binding between human immunoglobulin G (IgG) and *Staphylococcus aureus* protein A (SpA), we demonstrate the high sensitivity and usefulness of the QCM developed here. Second, we investigate the effect of the electrode on the QCM sensitivity by solving a five-layered oscillator model. The electrode causes two critical problems; it deteriorates the QCM sensitivity, and it limits the use of the Sauerbrey equation. QCM results have been analyzed on the basis of the Sauerbrey equation, which, however, does not apply to thinner oscillators with gold electrodes. Thus, we have to discuss the applicability of the Sauerbrey equation. Third, we investigate the effect of the flow rate in the range between 50 and 1000 μL/min on the sensitivity and affinity using the QCM flow injection system. These results indicate that the flow rate highly affects the sensitivity but does not affect the apparent affinity.

VIBRATIONAL ANALYSIS OF MULTILAYERED QCM

The Sauerbrey equation[16] estimates the frequency change Δf caused by adsorption of a mass Δm on the oscillator surface by $\Delta f = -f\Delta m/M_q$, where M_q denotes the mass of the quartz crystal. Thus, there is a linear relationship between the adsorbed mass and the frequency change, which has been used for quantitative analysis of QCM results. The Sauerbrey equation gives

$$\Delta f = -\frac{\rho_s v_q}{2\rho_q}\frac{1}{d_q^2} \tag{1}$$

Here, v_q, ρ_q, and d_q are the shear-wave velocity, the mass density, and the thickness of the quartz crystal, respectively. ρ_s denotes the area mass density of the adsorbed substance. Therefore, the QCM sensitivity $|\Delta f|$ is inversely proportional to the square of the thickness of the oscillator, and it is obvious that thinner oscillator provides higher sensitivity. (We neglected the viscosity effect in this study because we used much higher frequencies than conventional QCMs.) Equation 1 shows good agreement with measurements when the oscillator is thick enough compared with the electrode thickness. However, thinning the oscillator increases the inertia resistance of the electrode layers and causes elastic coupling of the acoustic wave with protein layers,[11] leading to discrepancy from the Sauerbrey equation.[12] Especially, Au films were usually used as electrodes because of their high association with thiol compounds, but the mass density of Au is considerably larger than that of α-quartz by a factor 7.3, causing very high inertia resistance at the oscillator surfaces, where the vibrational acceleration takes the maximum.

We then have to investigate the limitation of the Sauerbrey equation in the use of a thinner QCM. When both surfaces are used as the QCM sensor, the oscillator consists of five layers: middle α-quartz layer, two electrodes layers sandwiching it, and two protein layers adsorbed on the electrodes. However, our previous calculations assumed three layers for the one-side use for simplicity. We here propose more generalized vibrational analysis for plane-shear-wave resonances in a multilayer system consisting of n layers as shown in Figure 1. The partial waves in individual layers are expressed by

$$u_i^{(\pm)} = A_i^{(\mp)} e^{\mp jk_i z} \tag{2}$$

where u_i and A_i denote the horizontal displacement and the complex amplitude in the ith layer, respectively. (The term $e^{j\omega t}$ is omitted.) $j = \sqrt{-1}$. The superscripts (+) and (−) denote

(18) Kanazawa, K.; Gordon, J. *Anal. Chem.* **1985**, *57*, 1770–1771.
(19) Martin, S.; Granstaff, V.; Frye, G. *Anal. Chem.* **1991**, *63*, 2272–2281.
(20) Höök, F.; Kasemo, B.; Nylander, T.; Fant, C.; Sott, K.; Elwing, H. *Anal. Chem.* **2001**, *73*, 5796–5804.
(21) Su, X.; Lin, C.-Y.; O'Shea, S. J.; Teh, H. F.; Peh, W.; Thomsen, J. S. *Anal. Chem.* **2006**, *78*, 5552–5558.
(22) Spangler, B. D.; Wilkinsona, E. A.; Murphyb, J. T.; Tylerb, B. J. *Anal. Chim. Acta* **2001**, *444*, 149–161.
(23) Ogi, H.; Motohisa, K.; Hatanaka, K.; Ohmori, T.; Hirao, M.; Nishiyama, M. *Jpn. J. Appl. Phys.* **2007**, *46*, 4693–4697.

quantities for downward and upward partial plane waves, respectively. k_i is the wavenumber at the ith layer given by

$$k_i = 2\pi f\sqrt{\frac{\rho_i}{G_i}} \tag{3}$$

Here, G_i and ρ_i are the shear modulus and the mass density at the ith layer, respectively. The boundary conditions for continuity of the displacement and the shear stress are as follows:

$$G_1\left(\frac{\partial u_1^{(+)}}{\partial z} + \frac{\partial u_1^{(-)}}{\partial z}\right) = 0 \quad \text{at} \quad z = 0 \tag{4}$$

$$G_n\left(\frac{\partial u_n^{(+)}}{\partial z} + \frac{\partial u_n^{(-)}}{\partial z}\right) = 0 \ \text{at} \ z = \mathrm{D}_n \tag{5}$$

$$u_i^{(+)} + u_i^{(-)} = u_{i+1}^{(+)} + u_{i+1}^{(-)} \qquad \text{at} \ z = D_i \tag{6}$$

and

$$G_i\left(\frac{\partial u_i^{(+)}}{\partial z} + \frac{\partial u_i^{(-)}}{\partial z}\right) = G_{i+1}\left(\frac{\partial u_{i+1}^{(+)}}{\partial z} + \frac{\partial u_{i+1}^{(-)}}{\partial z}\right) \quad \text{at} \ z = D_i \tag{7}$$

Here, D_i is the distance of the ith interface from the top surface (Figure 1). Substitution of eq 2 into eqs 4–7 falls into an eigenvalue problem $\Gamma\mathbf{A} = 0$ with a matrix Γ of $(2n) \times (2n)$. The vector $\mathbf{A} = (A_1^{(+)}, A_2^{(+)}, \cdots, A_n^{(+)}, A_1^{(-)}, A_2^{(-)}, \cdots, A_n^{(-)})^{\mathrm{T}}$ consists of the complex amplitudes. Thus, resonance frequencies of the multilayer are obtained from eigenvalues of Γ by solving $\det[\Gamma] = 0$, from which we exactly calculated the resonance frequency for actual QCM oscillators.

This analytical method is generally applicable to many QCM experiments, including detection on both surfaces with multiprotein layers. Of course, it applies to the five-layer oscillator in the present study, and we calculated the frequency change for $n = 5$.

EXPERIMENTAL SECTION

Surface Preparation. A 30-μm-thick AT-cut quartz plate with 5×4 mm^2 was used, whose fundamental resonance frequency was near 55 MHz. It was cleaned in a piranha solution (98% H_2SO_4: 33% H_2O_2 = 7:3), and 18-nm Au thin films were deposited after 2-nm Cr thin films on both surfaces by the magnetron sputtering method for the subsequent gold−alkanethiol binding reaction. (The 20-nm-thin films hardly affect the sensitivity and the availability of the Sauerbrey equation, as shown later.) It was cleaned again in the piranha solution, rinsed with ultrapure water several times, and immersed in a 10 mM 10-carboxy-1-decanethiol/absolute ethanol solution for 20 h at 4 °C. After rinsing with absolute ethanol three times, the oscillator was set in the handmade sensor cell[11,12] by softly sandwiching a part of the edge by silicon rubber sheets. The QCM cell was then installed in the home-built flow injection system as shown in Figure 2, and the immobilization of SpA was performed in the flow injection system as follows. The resonance frequency was monitored in a noncontacting manner as will be shown later until the fractional-frequency variation was smaller than 10^{-6}, while the phosphate

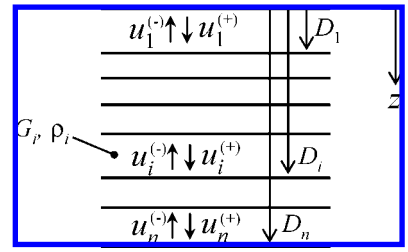

Figure 1. Partial plane waves propagating in a multilayered oscillator.

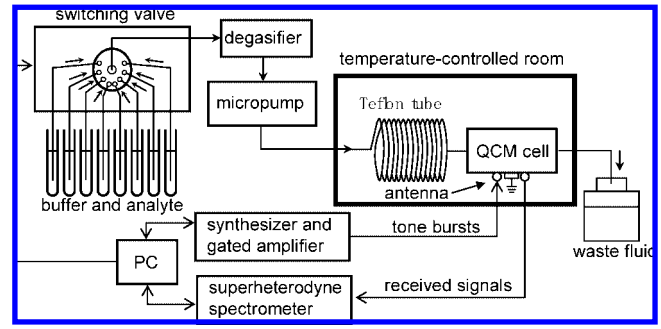

Figure 2. Home-built wireless−electrodeless QCM system.

buffer solution (PBS; pH 7.4) flowed at a rate of 200 μL/min as a carrier buffer. Then, the solutions of 100 mM 1-ethyl-3-(3-dimethylaminopropyl)carbodiimide, hydrochloride (EDC) and 0.4 mg/mL SpA/PBS were injected for 1 h to activate the carboxyl terminals and immobilize SpA molecules. A 10 mg/mL bovine serum albumin (BSA) solution was then injected for blocking the remaining activated sites to avoid nonspecific binding of IgG, which was followed by injections of analyte solutions.

Human IgG was from Athens Research and Technology, Inc. (product 16-16-090707; purity ~95%). SpA was from Zymed Laboratories, Inc. (product 10-1100; purity 98%). 10-Carboxy-1-decanethiol (product C385) and EDC (product W001) were from Dojindo Laboratories. BSA (90480608) were from Sigma-Aldrich Japan. All of other chemicals were purchased from Wako Pure Chemical Industries Ltd.

Experimental Procedure. The micropump (Uniflows Co. Ltd., model 3005FSB2) provided a steady flow of the PBS carrier solution. The switching valve (FLOM Co., Ltd., model 401) selected one analyte solution to be injected among eight vials, which flowed into the sensor cell through the degasifier (Uniflows Co. Ltd., model DG-7101). The 3-m Teflon tube column made the solution temperature stable at a set value (37 °C). Tone bursts were applied to the generation antenna to generate shear-horizontal vibration of the quartz in a noncontacting manner.[24] After the excitation, the detection antenna received reverberation signals, which entered into the superheterodyne spectrometer (RITEC Inc., model SNAP-1-100) to measure the phase and amplitude of the received signals using the driving signal as the reference.[25] Frequency scanning determined resonance frequency from peak-amplitude frequency, which was repeated until resonance frequency became sufficiently stable. We then monitored the phase of the signal to make a quick measurement (~0.1 s).

(24) Ogi, H.; Niho, H.; Hirao, M. *Appl. Phys. Lett.* **2006**, *88*, 141110.
(25) Hirao, M.; Ogi, H. *EMATs for Science and Industry: Noncontacting Ultrasonic Measurements*; Springer/Kluwer: Boston, 2003.

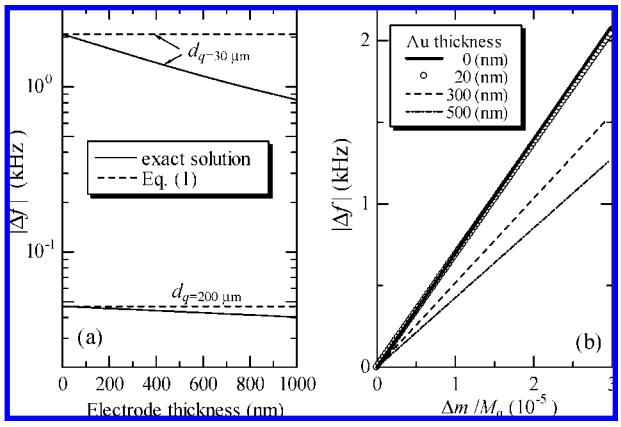

Figure 3. (a) Amount of the frequency change caused by the adsorption of 1-nm protein layers on both surfaces on Au electrodes. Solid curves are the exact solutions for five-layered oscillators, and broken lines are the predictions from the Sauerbrey equation. (b) Amount of the frequency change caused by the increase of the thickness (or mass) of the protein layers for a 30-μm-thick oscillator with various electrode thicknesses.

The frequency change was determined from the linear relationship between frequency and phase around a resonance.[12]

The IgG solutions were injected after the blocking procedure. The typical injection sequence is shown below: (i) injection of an IgG solution, (ii) injection of PBS, (iii) injection of glycine−HCl buffer (GHB) solution (0.1 M, pH 2.4) to dissolve the IgG−SpA binding, (iv) injection of PBS, and (v) injection of the next IgG solution (returning to (i)). The concentration of IgG and the flow rate were changed to investigate their influence on sensitivity and affinity.

RESULTS AND DISCUSSION

Electrode Effect. We investigated theoretically the influence of the electrodes on the QCM response in the detection of a typical protein. The protein layer of 1 nm was assumed, simulating a human-IgG layer. (IgG molecule measures near 1 nm along its longitudinal direction.[26]) Figure 3a shows the frequency change calculated for adsorption of the 1-nm protein layers on both surfaces. We assumed the shear modulus and the mass density of outer protein layers to be 0.1 GPa and 1500 kg/m^3, respectively, and we used G_q =29 GPa and ρ_q =2650 kg/m^3 for AT-cut quartz[27] and G_{Au} = 28 GPa and ρ_{Au} =19 284 kg/m^3 for Au layers. Broken lines in Figure 3a are the estimation with the Sauerbrey equation (eq 1). For a conventional QCM sensor with a 200-μm-thick quartz plate, deposited electrodes little affect the sensitivity, and the difference of the actual frequency change from the Sauerbrey prediction is marginal. However, when the quartz thickness becomes smaller, the sensitivity increases, but the presence of electrode layers deteriorates the sensitivity. For example, a 30-μm-thick electrodeless QCM can cause 2.08-kHz frequency change, but this value becomes 1.27 kHz when 500-nm-thick Au electrodes are present (Figure 3a). Therefore, 500-nm-thick electrodes on surfaces of a 30-μm-thick-quartz plate decrease the QCM sensitivity by 40%. Thus, the electrodes significantly deteriorate the QCM sensitivity when the oscillator becomes thinner. Figure 3b shows the calculation of the change in the resonance frequency caused by the adsorption of the IgG molecules. The sensitivity of the 30-μm-thick QCM is again lowered only by the electrodes. Furthermore, the Sauerbrey equation cannot be applied for thicker electrodes, lowering the reliability of the thermodynamic analysis for affinity. It neglects the contributions of the electrode mass and electrode stiffness to the resonance frequency, which however become significant as the oscillator becomes thinner. Actually, panels a and b in Figure 3 show that the frequency change is dependent on the electrode thickness. The Sauerbrey equation estimates the maximum frequency change, and it cannot predict accurate frequency change as the electrode thickness increases. Thus, the electrodeless approach is an important key for achieving high-sensitivity and quantitative QCM biosensors.

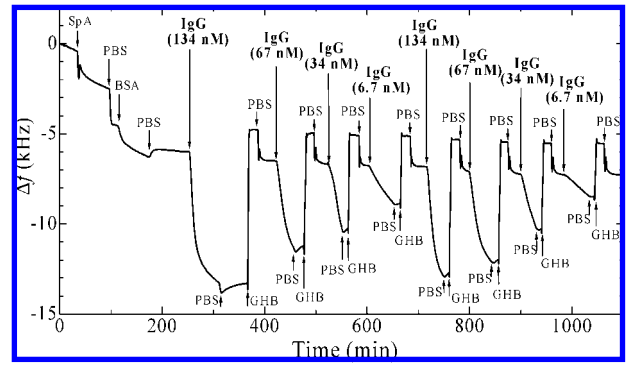

Figure 4. As-measured frequency response for an injection sequence. Arrows indicate the arrival time of solutions at the sensor cell.

In the present study, we used 20-nm-thick Au/Cr films; their effects on the sensitivity and the Sauerbrey equation can be neglected from the results of Figure 3a and b.

Repeatability of the Sensor. We used one sensor tip for many measurements of the interaction between IgG and SpA, and the repeatability was confirmed in advance. Figure 4 shows the typical as-measured frequency response for an injection sequence. The resonance frequency decreased exponentially when the IgG solution reached the QCM cell. After the injection of the glycine−HCl buffer (GHB) solution, the resonance frequency increased beyond the baseline, but it recovered by the injection of PBS. The sensor tip then showed nearly identical performance. Panels a and b in Figure 5 show binding curves observed for IgG solutions of different concentrations between 67 pM and 67 nM. The binding reaction is clearly observed even for a low-concentration solution after several dissociation procedures. The repeatability was well confirmed for 20 injections for a single sensor tip. We used a sensor tip for ~10 measurements and replaced it with a new tip. The typical fluctuations of the amount of the frequency decrement and that of the exponential coefficient value (α) for the same concentration IgG solution were within 20 and 15%, respectively.

Kinetic Analysis. Resonance-frequency change can be incorporated in the chemical kinetics theory when three assumptions are satisfied. First, the reaction occurs with a pseudo-first-order manner. Second, the concentration of the injected IgG solution

(26) Sarma, V.; Silverton, E.; Davies, D.; Terry, W. *J. Biol. Chem.* **1971**, *246*, 3753–3759.
(27) Ogi, H.; Ohmori, T.; Nakamura, N.; Hirao, M. *J. Appl. Phys.* **2006**, *100*, 053511.

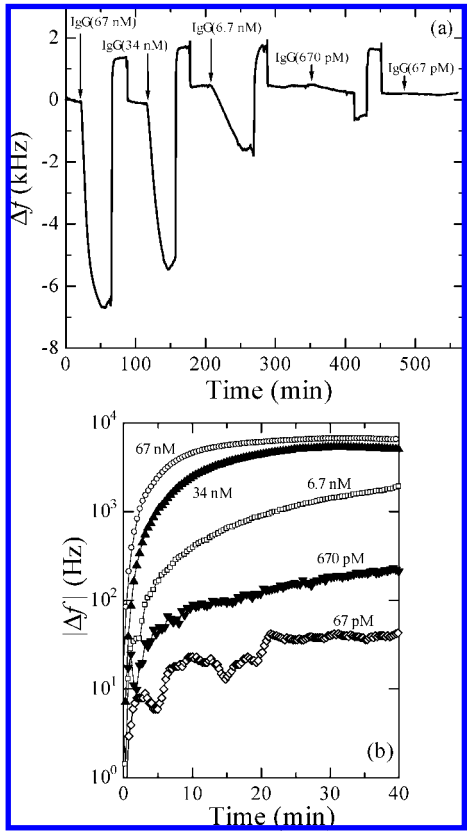

Figure 5. (a) As-measured frequency response and (b) binding curves for injections of IgG solutions of various concentrations between 67 pM and 67 nM. Note that a logarithmic scale is used in (b).

remains unchanged throughout the reaction. Third, the Sauerbrey equation is satisfied; that is, the amount of the frequency shift is proportional to the amount of the adsorbed IgG molecules on protein A. Based on these assumptions, the relationship between the frequency change and the kinetics of the binding reaction has been formulated as[10,17]

$$\Delta f(t) = \Delta f_e(e^{-\alpha t} - 1) \tag{8}$$

$$\alpha = k_a C_{IgG} + k_d \tag{9}$$

Here, Δf_e is the frequency change at the equilibrium state. C_{IgG} is the concentration of IgG. k_a and k_d are association rate and dissociation rate constants, respectively. The equilibrium constant K_A given by

$$K_A = \frac{k_a}{k_d} \tag{10}$$

indicates the affinity between the two molecules. Equations 8 and 9 show that the frequency change obeys the exponential function and the exponential coefficient is proportional to C_{IgG}. Therefore, plotting α versus C_{IgG} provides a line whose slope and intercept provide k_a and k_d, respectively; their ratio yields K_A.

Hindrance Effect and Kinetic Constants. Figure 6 shows binding curves for injections of IgG solutions of various concentrations. Solid lines are the fitted theoretical function (eq 8). When the IgG solution arrives at the sensor cell, the frequency starts to

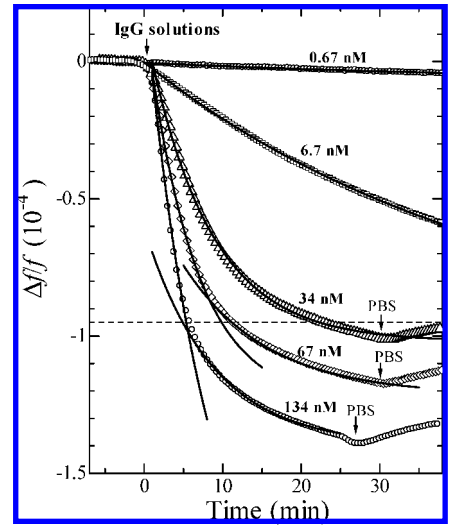

Figure 6. Binding curves for injections of IgG solutions of various concentrations. The solid curves are fitted theory (eq 8). The horizontal broken line indicates the critical value, by which the steric hindrance effect becomes significant and decreases the affinity.

decrease exponentially, and the theoretical function in eq 8 completely fits the frequency change for lower-concentration solutions. Thus, the three assumptions made above are essentially validated. However, for higher-concentration solutions (C_{IgG} > 34 nM), a single-exponential function fails to fit the observed frequency change, and two exponential functions are apparently required to explain the frequency change. The critical value, at which the frequency change departs from the first exponential function, appears around $\Delta f/f = 9.5 \times 10^{-5}$ ($\Delta f = 5.2$ kHz).

This critical value can be consistently explained from the steric hindrance effect of IgG molecules: The Sauerbrey equation converts the critical value into the adsorbed mass of the IgG molecules on the quartz surfaces of 1.5×10^{-7} g, corresponding to the total number of molecules of 6.1×10.[11] The effective area of the QCM sensor is $5 \times 4 \times 2$ mm^2, which yields the occupation area of a single molecule (66 nm^2), and the diameter of the equivalent sphere of 9.2 nm. On the other hand, the volume of a single IgG molecule is about $14.2 \times 3.8 \times 4.5$ nm^3,[26] corresponding to the equivalent sphere with a diameter of 7.7 nm. These two representative diameters are in good agreement, despite involving no ambiguous parameters. Therefore, at the critical point, almost the whole surfaces of the oscillator were covered by IgG molecules, and the steric hindrance subsequently occurred, resulting in deceleration of binding affinity because of buried binding sites of protein A.

This result gives an important indication of the determination of kinetic constants using a flow injection system. Previous QCMs used only one side of their oscillators, and when the conventional 9-MHz QCM is used, for example, the critical value will be $\Delta f/f = -0.78 \times 10^{-5}$ or $\Delta f = -70$ Hz. Therefore, the affinity evaluation must be performed using small frequency changes; otherwise, the affinity value is underestimated. Furthermore, not only QCMs but also SPR immunoassays adopted flow injection systems to evaluate the kinetics of biomolecule reactions, and they have to use low-concentration analyte solutions or physical responses before the steric hindrance effect becomes dominant.

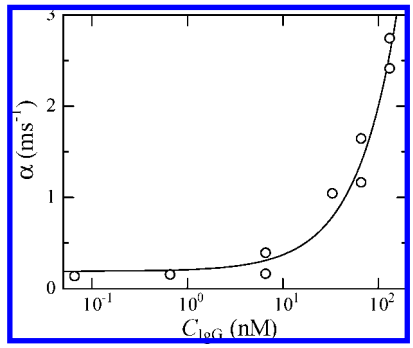

Figure 7. Langmuir plot for the concentration of IgG (C_{IgG}) versus the exponential coefficient (α) to determine the kinetic constants. The solid line denotes the fitted theoretical function (eq 9). Note that a logarithmic scale is used for the horizontal axis. The flow rate was 500 μL/min.

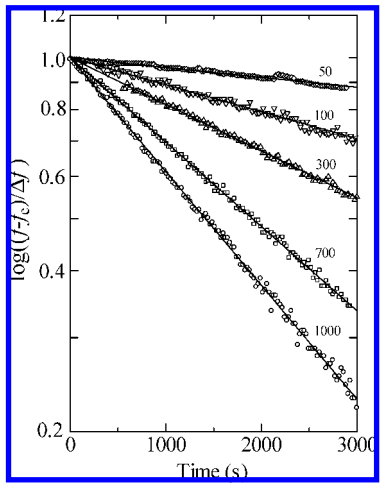

Figure 8. Frequency responses for injection of 6.7 nM IgG solution at various flow rates. The logarithmic scale is used. The solid lines are fitted theoretical functions (eq 8), showing good agreement with measurements. The numbers denote the flow rate in μL/min.

We thus determined the affinity value using the data below the critical frequency change. Figure 7 shows the relationship between α and C_{IgG}. The solid line represents the theory, giving k_a, k_d, and K_A.

Effects of Flow Rate. Increasing the flow rate considerably accelerated the binding reaction as shown in Figure 8. We investigated the effect of the flow rate on the kinetic constants between 50 and 1000 μL/min, corresponding to flow velocities between 0.11 and 2.22 mm/s in the sensor cell, respectively. Figure 9 shows the result. Both association and dissociation kinetic constants, k_a and k_d, increase as the flow rate increases.

We attribute this observation to the variation of the local concentration of the analyte. As the binding reaction progresses, the concentration of the analyte locally decreases near the interaction surface, and it must recover in a time shorter than the reaction time; otherwise, the apparent association constant decreases because the analyte concentration is lowered. Similarly, the local concentration of the analyte near the surface is increased in the progress of the dissociation reaction in a later stage, leading to decrease of the apparent dissociation constant. Therefore, the concentration variation of the surrounding solution should be minimized. Self-diffusion of biomolecules in liquids is, however,

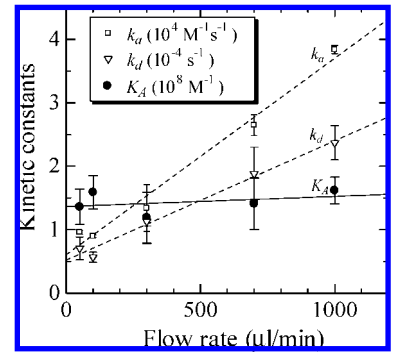

Figure 9. Correlations of the association rate constant k_a, the dissociation rate constant k_d, and the equilibrium constant K_A with the flow rate.

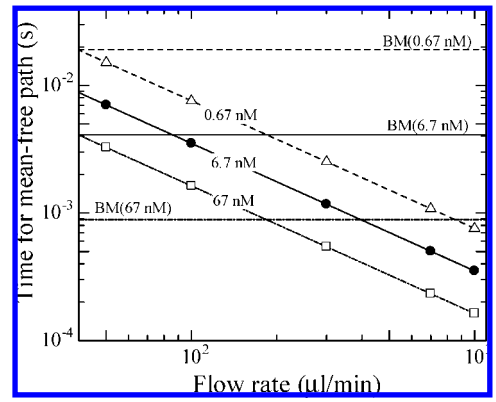

Figure 10. Relationship between the flow rate and the time for an IgG molecule to move to the mean-free path. BM denotes the movement by Brownian motion.

insufficient to make the concentration stable because of their larger molecular masses. To confirm this, we calculate the time needed for a molecule to move to the mean-free path. According to the Einstein equation for Brownian motion,[28] the average distance σ for a molecule to move in time t due to Brownian motion is given by $\sigma = \sqrt{2Dt}$. D denotes the diffusion coefficient and is reported to be 7.4×10^{-11} m^2/s for an IgG molecule in liquid.[29] Thus, the time needed to move to the mean-free path is calculated when the analyte concentration is known. (We estimated the mean-free path as the average distance between molecules.) This time is compared with that caused by the flow of the analyte in Figure 10. The time to carry an IgG molecule to the mean-free path by the flow decreases as the flow rate increases, and it is largely shorter than that caused by Brownian motion. For an analyte concentration of 0.67 nM, for example, flow significantly contributes to keep the concentration unchanged. Thus, a larger flow rate is required to increase the sensitivity and make the kinetic analysis appropriate. A more important observation is that the equilibrium constant K_A is nearly independent of the flow rate (Figure 9), because the flow effect is canceled by taking a ratio between k_a and k_d. This conveniently justifies affinity values determined by QCM and SPR methods in the past, although the association and dissociation constants would include serious errors.

(28) Einstein, A. *Ann. Phys.* **1905**, *17*, 549–560.
(29) Karlsson, D.; Zacchi, G.; Axelsson, A. *Biotechnol. Prog.* **2002**, *18*, 1423–1430.

CONCLUSION

The 55-MHz wireless−electrodeless QCM showed high sensitivity in the detection of IgG solution by protein A immobilized on both surfaces of the 30-μm-thick oscillator. The binding curves were obtained for IgG solutions of concentrations between 67 pM and 134 nM, which well agreed with the chemical kinetic theory.

The electrode effect was investigated for five-layered oscillators, which demonstrated significant influence of the Au electrodes on the sensitivity and the availability of the Sauerbrey equation. For example, 500-nm-thick Au films on both surfaces decrease the sensitivity by 40%.

The critical frequency values for the steric hindrance effect were −5.2 kHz for the 30-μm-thick (55-MHz) oscillator and −70 Hz for a conventional 9-MHz oscillator, respectively. Under these values, the apparent affinity value is decreased.

As the flow rate increased, both association and dissociation constants increased by a factor of about 3 between 50 and 1000 μL/min. Comparing the Brownian motion effect with the flow effect using the Einstein relationship, it was revealed that the Brownian motion was insufficient to keep the concentration of the surrounding analyte constant and the flow rate governed the reaction rate. However, the equilibrium constant K_A remained unchanged, indicating that previously reported affinity values using QCMs and SPRs with the flow injection system are valid.

ACKNOWLEDGMENT

A part of this study was supported by Life Phenomena and Measurement Analysis, PRESTO, by Japan Science and Technology Agency.

Received for review March 5, 2008. Accepted May 14, 2008.

AC800459G